SPACE WEATHER, VOL. 9, S00E11, doi:10.1029/2009SW000564, 2011

Transmission of galactic cosmic rays through Mars atmosphere

L. W. Townsend,[1] M. PourArsalan,[1] F. A. Cucinotta,[2] M. Y. Kim,[2] and N. A. Schwadron[3]

Received 26 December 2010; accepted 31 May 2011; published 29 June 2011.

[1] For human operations on the surface of Mars, methods of estimating radiation exposures from galactic cosmic rays (GCRs) are needed. To facilitate making estimates of human radiation exposures for crew operations in the Martian atmosphere, lookup tables have been generated that provide doses for critical body organs and effective doses for exposures from galactic cosmic rays anywhere on the surface of Mars. The organ doses and effective doses are tabulated for carbon dioxide atmospheric shielding areal densities ranging from 0 to 300 g cm^{-2} followed by aluminum spacecraft or habitat shield areal densities ranging from 0 to 100 g cm^{-2}. The Badhwar-O'Neill GCR model for interplanetary magnetic field potentials, ranging from the most probable solar minimum (currently 417 MV) to solar maximum conditions (1800 MV) in the solar cycle, is used as input into the calculations. This model is the standard one used for space operations at the Space Radiation Analysis Group at NASA Johnson Space Center. Use of the tables is illustrated for an environment consisting of the current galactic cosmic radiation spectrum impinging on an aluminum habitat on the surface of Mars.

Citation: Townsend, L. W., M. PourArsalan, F. A. Cucinotta, M. Y. Kim, and N. A. Schwadron (2011), Transmission of galactic cosmic rays through Mars atmosphere, *Space Weather*, *9*, S00E11, doi:10.1029/2009SW000564.

1. Introduction

[2] Exposures of interplanetary crews on missions beyond low-Earth orbit have been the subject of various studies over the past several decades. A representative listing of these studies are presented in the references [*Baker et al.*, 2007; *Cucinotta and Durante*, 2006; *Hoff et al.*, 2002, 2004; *Kim et al.*, 2007, 2009; *Lyne and Townsend*, 1998; *Parsons and Townsend*, 2000; *Saganti et al.*, 2004; *Shinn et al.*, 1994; *Simonsen et al.*, 1990, 1991; *Townsend et al.*, 1989, 1991, 1992, 1994, 2006; *Townsend*, 2005; *Zapp et al.*, 2002]. The main objective of the Earth-Moon-Mars Radiation Exposure Module (EMMREM) framework is to provide researchers with the capability to characterize time-dependent radiation exposures in the Earth-Moon-Mars and interplanetary space environments. An overview of this framework is provided elsewhere [*Schwadron et al.*, 2010] as are examples of its application to galactic cosmic ray (GCR) [*Townsend et al.*, 2010] and solar energetic particle event (SEP) exposures [*PourArsalan et al.*, 2010] in interplanetary space.

[3] In this work we focus on the capabilities of the EMMREM framework to estimate GCR radiation exposures anywhere on the surface of Mars. To facilitate making estimates of human radiation exposures for crew operations in these scenarios, lookup tables have been generated that provide the means for obtaining estimates of doses for critical body organs and effective doses for exposures from GCR environments anywhere on the surface of Mars at any time during the solar cycle. A lookup table is used because the radiation environments are transported through as much as 500 g/cm^2 of atmosphere, aluminum and body self-shielding materials. Calculations at such depths for these complex space radiation environments cannot be carried out in near real time simulations. In section 2, the computational methods and models used to generate the lookup tables are described. Section 3 presents a discussion of the lookup tables and describes how to use them. Section 4 presents sample results for a Mars surface scenario involving a surface habitat for the current GCR environment to illustrate use of the tables. Finally, the paper finishes with concluding remarks in section 5.

2. Computational Methods and Models

[4] In this section the methods and models used to generate the lookup tables are presented. The transport of

[1]Department of Nuclear Engineering, University of Tennessee, Knoxville, Tennessee, USA.
[2]NASA Lyndon B. Johnson Space Center, Houston, Texas, USA.
[3]Department of Astronomy, Boston University, Boston, Massachusetts, USA.

the incident radiation spectra is carried out using the space radiation transport code HZETRN [*Nealy et al.*, 2007] for the incident galactic cosmic ray spectra. The spectra are transported through the Mars atmosphere (0 to 300 g cm^{-2}), then through aluminum shielding (0 to 100 g cm^{-2}), and finally through water to simulate the body self-shielding for the organ of interest. For the body composition, water is commonly used as a substitute for soft tissue. A realistic body self shielding distribution, based upon the Computerized Anatomical Male (CAM) model of human geometry [*Billings and Yucker*, 1973] is used to estimate organ doses and dose equivalents. These are then used to calculate the effective dose, which is the relevant radiation protection quantity for comparing to the current exposure limits, as specified in the NASA Permissible Exposure Limits (PELs) [*NASA*, 2007]. The body organ self-shielding distributions are obtained using 968 rays penetrating the body, which cover the entire 4π solid angle surrounding a particular body organ site. Doses and organ dose equivalents are calculated for the bone marrow, brain, bladder, breast, colon, esophagus, heart, kidney, eye lens, liver, lung, gonads, pancreas, skin, stomach, and thyroid. For the skin and bone marrow, which are distributed throughout the body, doses and dose equivalents are obtained by averaging over more than 40 anatomical locations for each organ. For large organs, such as the lung, kidney, etc, multiple sites in the organ are averaged over. For localized organs, such as the eye lens, only one site is used. Note that organ doses (D) are given in units of centigray (cGy), where 1cGy = 0.01 Gy = 1 rad and 1 Gy = 1 J/kg. Organ dose equivalents (H) are in units of centisievert (cSv) where 1cSv = 0.01 Sv = 1 rem and 1Sv = 1 J/kg. The units on effective dose (E) are also cSv.

[5] Organ doses are calculated by folding the body organ self-shielding distribution with the dose as a function of depth in water obtained from the applicable transport code using

$$D(x) = \sum_j \int_0^\infty S_j(E)\Phi_j(x,E)dE \quad (1)$$

where D(x) is the dose at depth x in water due to all particles, S_j (E) is the stopping power in water of particles of type j with energy E, and Φ_j (x, E) is the flux of particles of type j at x with energy E. The organ dose equivalents are similarly obtained from the transport code using

$$H(x) = \sum_j \int_0^\infty Q_j(E)S_j(E)\Phi_j(x,E)dE \quad (2)$$

where Q is a quality factor that accounts for the fact that different particle types do differing amounts of biological damage for the same absorbed dose. Once the organ dose equivalents are calculated for each organ, the effective dose is obtained from

$$E = \sum_T w_T H_T \quad (3)$$

In equation (3) the tissue weighting factors w_T are the proportionate detriment of the organ denoted by T when the whole body is irradiated. The w_T values used herein are listed in Table 5.1 in report 116 of the National Council on Radiation Protection and Measurements [*National Council on Radiation Protection and Measurements*, 1993].

[6] The calculations presented in the lookup tables use the latest GCR environmental model of Badhwar and O'Neill [*O'Neill*, 2006], which is the current NASA standard. The incident spectra that are transported through the three layers of material (atmosphere, aluminum and water) include all elements from hydrogen through iron, which are the major ones contributing to human exposures in space. Incident GCR spectra were generated for a variety of interplanetary magnetic field potentials ranging from 417 MV (current environment) to 1800 MV. These span the range of potentials likely to be encountered (417, 450, 500, 600, 700, 800, 900, 1000, 1100, 1200, 1300, 1400, 1500, 1600, 1700, and 1800 MV).

3. Lookup Tables: Description and Use

[7] For each incident GCR environment, as specified by its interplanetary magnetic field potential, tables were generated for organ doses, organ dose equivalents, and for effective dose for 150 combinations of Mars atmosphere thicknesses (0 to 300 g cm^{-2}) and aluminum shielding thicknesses (0 to 100 g cm^{-2}). For the CO_2 atmosphere of Mars and the aluminum shielding, the "thicknesses" are in units of areal density (g cm^{-2}) where *areal density* (*g* cm^{-2}) = *density* (*g* cm^{-3}) × *thickness* (*cm*). The Mars atmosphere thicknesses in the lookup tables are 0, 1, 2, 4, 5, 10, 15, 20, 30, 40, 60, 80, 100, 150 and 300 g cm^{-2}. For the aluminum, the thicknesses are 0, 0.3, 1, 5, 10, 20, 30, 40, 60 and 100 g cm^{-2}.

[8] The complete set of lookup tables is available from the Boston University website: http://www.bu.edu/csp/EMMREM/tables/gcr_doses_mars.txt http://www.bu.edu/csp/EMMREM/tables/gcr_dose_equivalents_mars.txt.

3.1. Description of GCR Tables

[9] As described above, lookup tables for the incident GCR environments displaying organ doses, organ dose equivalents, and effective doses are available. Table 1 displays a portion of the lookup table, taken from the Boston University website, for organ dose (skin, eye, bone marrow (also sometimes referred to as blood-forming organs) brain (central nervous system), and heart) and effective dose for each combination of Mars atmosphere and aluminum shielding areal densities ("thicknesses") for the current (2009) GCR environment (417 MV inter-

Table 1. Sample GCR Dose and Effective Dose Lookup Table[a]

Phi (MV)	Mars Atmosphere (g/cm^2)	Aluminum (g/cm^2)	Skin Dose (cGy/day)	Eye Dose (cGy/day)	Bone Marrow (BFO) Dose (cGy/day)	CNS (Brain) Dose (cGy/day)	Heart Dose (cGy/day)	Effective Dose (cSv/day)
417	0.0	0.0	0.0442	0.0684	0.0621	0.0642	0.0410	0.2040
417	0.0	0.3	0.0673	0.0680	0.0620	0.0641	0.0409	0.2045
417	0.0	1.0	0.0677	0.0680	0.0619	0.0640	0.0408	0.2013
417	0.0	5.0	0.0671	0.0671	0.0612	0.0632	0.0404	0.1861
417	0.0	10.0	0.0659	0.0659	0.0604	0.0623	0.0399	0.1729
417	0.0	20.0	0.0637	0.0636	0.0589	0.0606	0.0389	0.1569
417	0.0	30.0	0.0617	0.0617	0.0574	0.0590	0.0380	0.1482
417	0.0	40.0	0.0599	0.0599	0.0561	0.0576	0.0372	0.1432
417	0.0	60.0	0.0566	0.0566	0.0535	0.0548	0.0355	0.1383
417	0.0	100.0	0.0506	0.0507	0.0484	0.0495	0.0321	0.1330
417	1.0	0.0	0.0335	0.0338	0.0309	0.0319	0.0204	0.0997
417	1.0	0.3	0.0337	0.0338	0.0308	0.0319	0.0204	0.0991
417	1.0	1.0	0.0337	0.0338	0.0308	0.0318	0.0203	0.0977
417	1.0	5.0	0.0333	0.0333	0.0305	0.0314	0.0201	0.0909
417	1.0	10.0	0.0328	0.0328	0.0301	0.0310	0.0199	0.0849
417	1.0	20.0	0.0317	0.0317	0.0293	0.0302	0.0194	0.0776
417	1.0	30.0	0.0307	0.0307	0.0286	0.0294	0.0190	0.0736
417	1.0	40.0	0.0299	0.0298	0.0280	0.0287	0.0185	0.0713
417	1.0	60.0	0.0282	0.0282	0.0267	0.0273	0.0177	0.0690
417	1.0	100.0	0.0252	0.0253	0.0241	0.0247	0.0160	0.0664
417	2.0	0.0	0.0333	0.0336	0.0307	0.0317	0.0203	0.0968
417	2.0	0.3	0.0335	0.0336	0.0307	0.0317	0.0203	0.0963
417	2.0	1.0	0.0335	0.0335	0.0307	0.0317	0.0203	0.0950
417	2.0	5.0	0.0331	0.0331	0.0303	0.0313	0.0201	0.0889
417	2.0	10.0	0.0326	0.0326	0.0300	0.0309	0.0198	0.0835
417	2.0	20.0	0.0316	0.0315	0.0292	0.0301	0.0194	0.0768
417	2.0	30.0	0.0306	0.0306	0.0286	0.0293	0.0189	0.0731
417	2.0	40.0	0.0298	0.0297	0.0279	0.0286	0.0185	0.0710
417	2.0	60.0	0.0281	0.0281	0.0266	0.0273	0.0176	0.0689
417	2.0	100.0	0.0251	0.0252	0.0241	0.0246	0.0160	0.0663
417	4.0	0.0	0.0329	0.0332	0.0305	0.0314	0.0201	0.0919
417	4.0	0.3	0.0331	0.0331	0.0305	0.0314	0.0201	0.0915
417	4.0	1.0	0.0331	0.0331	0.0304	0.0313	0.0201	0.0904
417	4.0	5.0	0.0328	0.0327	0.0301	0.0310	0.0199	0.0855
417	4.0	10.0	0.0323	0.0322	0.0298	0.0306	0.0197	0.0810
417	4.0	20.0	0.0313	0.0312	0.0291	0.0299	0.0192	0.0754
417	4.0	30.0	0.0304	0.0304	0.0284	0.0291	0.0188	0.0723
417	4.0	40.0	0.0295	0.0295	0.0277	0.0284	0.0184	0.0705
417	4.0	60.0	0.0280	0.0280	0.0265	0.0271	0.0175	0.0686
417	4.0	100.0	0.0250	0.0250	0.0239	0.0245	0.0159	0.0661
417	5.0	0.0	0.0327	0.0329	0.0303	0.0313	0.0201	0.0898
417	5.0	0.3	0.0329	0.0329	0.0303	0.0313	0.0200	0.0894
417	5.0	1.0	0.0329	0.0329	0.0303	0.0312	0.0200	0.0885
417	5.0	5.0	0.0326	0.0325	0.0300	0.0309	0.0198	0.0840
417	5.0	10.0	0.0321	0.0321	0.0296	0.0305	0.0196	0.0799
417	5.0	20.0	0.0312	0.0311	0.0290	0.0298	0.0192	0.0748
417	5.0	30.0	0.0303	0.0302	0.0283	0.0290	0.0188	0.0719
417	5.0	40.0	0.0294	0.0294	0.0277	0.0284	0.0183	0.0703
417	5.0	60.0	0.0279	0.0279	0.0264	0.0270	0.0175	0.0685
417	5.0	100.0	0.0249	0.0250	0.0239	0.0244	0.0158	0.0661
417	10.0	0.0	0.0318	0.0320	0.0298	0.0306	0.0197	0.0816
417	10.0	0.3	0.0320	0.0320	0.0298	0.0306	0.0197	0.0814
417	10.0	1.0	0.0320	0.0320	0.0297	0.0305	0.0197	0.0808
417	10.0	5.0	0.0318	0.0317	0.0295	0.0303	0.0195	0.0781
417	10.0	10.0	0.0314	0.0313	0.0292	0.0299	0.0193	0.0755
417	10.0	20.0	0.0306	0.0305	0.0285	0.0293	0.0189	0.0722
417	10.0	30.0	0.0298	0.0297	0.0279	0.0286	0.0185	0.0704
417	10.0	40.0	0.0290	0.0289	0.0273	0.0280	0.0181	0.0693
417	10.0	60.0	0.0274	0.0274	0.0260	0.0267	0.0173	0.0680
417	10.0	100.0	0.0245	0.0246	0.0235	0.0241	0.0156	0.0656
417	15.0	0.0	0.0311	0.0312	0.0293	0.0300	0.0194	0.0763
417	15.0	0.3	0.0313	0.0312	0.0293	0.0300	0.0194	0.0761
417	15.0	1.0	0.0313	0.0312	0.0292	0.0300	0.0194	0.0758
417	15.0	5.0	0.0311	0.0310	0.0290	0.0297	0.0192	0.0741

Table 1. (continued)

Phi (MV)	Mars Atmosphere (g/cm^2)	Aluminum (g/cm^2)	Skin Dose (cGy/day)	Eye Dose (cGy/day)	Bone Marrow (BFO) Dose (cGy/day)	CNS (Brain) Dose (cGy/day)	Heart Dose (cGy/day)	Effective Dose (cSv/day)
417	15.0	10.0	0.0308	0.0307	0.0287	0.0294	0.0190	0.0725
417	15.0	20.0	0.0300	0.0299	0.0281	0.0288	0.0186	0.0704
417	15.0	30.0	0.0293	0.0292	0.0275	0.0282	0.0183	0.0692
417	15.0	40.0	0.0285	0.0285	0.0269	0.0276	0.0179	0.0685
417	15.0	60.0	0.0270	0.0270	0.0257	0.0263	0.0170	0.0675
417	15.0	100.0	0.0241	0.0242	0.0232	0.0237	0.0154	0.0651
417	20.0	0.0	0.0305	0.0306	0.0288	0.0295	0.0191	0.0726
417	20.0	0.3	0.0306	0.0306	0.0288	0.0295	0.0191	0.0726
417	20.0	1.0	0.0306	0.0306	0.0288	0.0295	0.0191	0.0724
417	20.0	5.0	0.0305	0.0304	0.0286	0.0293	0.0189	0.0713
417	20.0	10.0	0.0302	0.0301	0.0283	0.0290	0.0188	0.0704
417	20.0	20.0	0.0295	0.0294	0.0277	0.0284	0.0184	0.0691
417	20.0	30.0	0.0288	0.0287	0.0272	0.0278	0.0180	0.0684
417	20.0	40.0	0.0281	0.0280	0.0266	0.0272	0.0176	0.0679
417	20.0	60.0	0.0266	0.0266	0.0253	0.0259	0.0168	0.0671
417	20.0	100.0	0.0237	0.0238	0.0228	0.0234	0.0152	0.0647
417	30.0	0.0	0.0294	0.0295	0.0280	0.0286	0.0186	0.0685
417	30.0	0.3	0.0295	0.0295	0.0280	0.0286	0.0186	0.0684
417	30.0	1.0	0.0296	0.0295	0.0280	0.0286	0.0186	0.0684
417	30.0	5.0	0.0295	0.0293	0.0278	0.0284	0.0184	0.0681
417	30.0	10.0	0.0292	0.0291	0.0275	0.0282	0.0183	0.0678
417	30.0	20.0	0.0286	0.0285	0.0270	0.0276	0.0179	0.0674
417	30.0	30.0	0.0279	0.0279	0.0264	0.0270	0.0175	0.0672
417	30.0	40.0	0.0272	0.0272	0.0259	0.0265	0.0172	0.0669
417	30.0	60.0	0.0258	0.0258	0.0246	0.0252	0.0164	0.0662
417	30.0	100.0	0.0230	0.0231	0.0221	0.0227	0.0147	0.0636
417	40.0	0.0	0.0285	0.0285	0.0273	0.0278	0.0181	0.0664
417	40.0	0.3	0.0286	0.0285	0.0273	0.0278	0.0181	0.0664
417	40.0	1.0	0.0286	0.0285	0.0272	0.0278	0.0181	0.0664
417	40.0	5.0	0.0285	0.0284	0.0271	0.0276	0.0180	0.0664
417	40.0	10.0	0.0283	0.0282	0.0268	0.0274	0.0178	0.0664
417	40.0	20.0	0.0277	0.0277	0.0263	0.0269	0.0175	0.0664
417	40.0	30.0	0.0271	0.0270	0.0257	0.0263	0.0171	0.0663
417	40.0	40.0	0.0264	0.0264	0.0252	0.0257	0.0167	0.0661
417	40.0	60.0	0.0250	0.0250	0.0239	0.0245	0.0159	0.0654
417	40.0	100.0	0.0222	0.0223	0.0215	0.0220	0.0142	0.0625
417	60.0	0.0	0.0268	0.0269	0.0259	0.0264	0.0172	0.0645
417	60.0	0.3	0.0270	0.0269	0.0259	0.0263	0.0172	0.0645
417	60.0	1.0	0.0269	0.0269	0.0258	0.0263	0.0172	0.0646
417	60.0	5.0	0.0269	0.0268	0.0257	0.0262	0.0170	0.0647
417	60.0	10.0	0.0266	0.0266	0.0254	0.0259	0.0169	0.0648
417	60.0	20.0	0.0261	0.0260	0.0249	0.0254	0.0165	0.0649
417	60.0	30.0	0.0255	0.0254	0.0243	0.0249	0.0162	0.0648
417	60.0	40.0	0.0248	0.0248	0.0238	0.0243	0.0158	0.0645
417	60.0	60.0	0.0235	0.0235	0.0225	0.0231	0.0150	0.0635
417	60.0	100.0	0.0207	0.0208	0.0201	0.0206	0.0133	0.0600
417	80.0	0.0	0.0253	0.0253	0.0245	0.0249	0.0163	0.0633
417	80.0	0.3	0.0254	0.0253	0.0245	0.0249	0.0163	0.0633
417	80.0	1.0	0.0254	0.0253	0.0244	0.0249	0.0162	0.0633
417	80.0	5.0	0.0253	0.0252	0.0243	0.0247	0.0161	0.0634
417	80.0	10.0	0.0251	0.0250	0.0240	0.0245	0.0160	0.0635
417	80.0	20.0	0.0245	0.0245	0.0235	0.0240	0.0156	0.0634
417	80.0	30.0	0.0239	0.0239	0.0229	0.0234	0.0152	0.0631
417	80.0	40.0	0.0232	0.0233	0.0224	0.0229	0.0148	0.0626
417	80.0	60.0	0.0219	0.0220	0.0211	0.0216	0.0140	0.0612
417	80.0	100.0	0.0192	0.0194	0.0187	0.0192	0.0124	0.0572
417	100.0	0.0	0.0237	0.0238	0.0231	0.0235	0.0154	0.0618
417	100.0	0.3	0.0239	0.0238	0.0231	0.0235	0.0154	0.0618
417	100.0	1.0	0.0238	0.0238	0.0231	0.0235	0.0153	0.0618
417	100.0	5.0	0.0237	0.0237	0.0229	0.0233	0.0152	0.0618
417	100.0	10.0	0.0235	0.0235	0.0226	0.0231	0.0150	0.0618
417	100.0	20.0	0.0229	0.0229	0.0221	0.0226	0.0147	0.0615
417	100.0	30.0	0.0223	0.0224	0.0215	0.0220	0.0143	0.0610
417	100.0	40.0	0.0217	0.0217	0.0209	0.0214	0.0139	0.0603

Table 1. (continued)

Phi (MV)	Mars Atmosphere (g/cm^2)	Aluminum (g/cm^2)	Skin Dose (cGy/day)	Eye Dose (cGy/day)	Bone Marrow (BFO) Dose (cGy/day)	CNS (Brain) Dose (cGy/day)	Heart Dose (cGy/day)	Effective Dose (cSv/day)
417	100.0	60.0	0.0204	0.0205	0.0197	0.0202	0.0131	0.0586
417	100.0	100.0	0.0178	0.0179	0.0173	0.0178	0.0115	0.0542
417	150.0	0.0	0.0200	0.0201	0.0196	0.0200	0.0130	0.0565
417	150.0	0.3	0.0201	0.0201	0.0196	0.0200	0.0130	0.0565
417	150.0	1.0	0.0200	0.0201	0.0196	0.0200	0.0130	0.0565
417	150.0	5.0	0.0199	0.0199	0.0194	0.0198	0.0129	0.0562
417	150.0	10.0	0.0197	0.0197	0.0191	0.0195	0.0127	0.0559
417	150.0	20.0	0.0191	0.0192	0.0186	0.0190	0.0124	0.0552
417	150.0	30.0	0.0185	0.0186	0.0180	0.0185	0.0120	0.0544
417	150.0	40.0	0.0179	0.0180	0.0175	0.0179	0.0116	0.0534
417	150.0	60.0	0.0167	0.0169	0.0163	0.0168	0.0109	0.0513
417	150.0	100.0	0.0144	0.0146	0.0142	0.0146	0.0094	0.0464
417	300.0	0.0	0.0107	0.0108	0.0107	0.0109	0.0071	0.0357
417	300.0	0.3	0.0107	0.0108	0.0107	0.0109	0.0071	0.0357
417	300.0	1.0	0.0107	0.0108	0.0106	0.0109	0.0071	0.0356
417	300.0	5.0	0.0105	0.0106	0.0105	0.0108	0.0070	0.0352
417	300.0	10.0	0.0104	0.0105	0.0103	0.0106	0.0069	0.0348
417	300.0	20.0	0.0100	0.0101	0.0100	0.0102	0.0066	0.0338
417	300.0	30.0	0.0096	0.0098	0.0096	0.0098	0.0064	0.0329
417	300.0	40.0	0.0093	0.0094	0.0092	0.0095	0.0061	0.0319
417	300.0	60.0	0.0085	0.0087	0.0085	0.0088	0.0057	0.0300
417	300.0	100.0	0.0072	0.0073	0.0072	0.0074	0.0048	0.026

[a]Here desc is GCR dose tables for Martian atmosphere.

planetary magnetic field potential). Table 1 includes entries for all GCR environments, arranged by their interplanetary magnetic field potentials, as listed above in the text (417 through 1800 MV).

3.2. Use of Tables

[10] The effective dose values in these tables can be used for comparison with the exposure limits in the NASA Permissible Exposure Limits guidelines to determine if the career exposure limits are being met for any scenario being investigated.

[11] 1. The entries for 0 g cm^{-2} in the Mars atmosphere column are appropriate for use in deep space, outside the atmosphere of Mars. The shadow shielding provided by the planet's bulk is not accounted for in these entries.

[12] 2. Table entries for thicknesses of 1 g cm^{-2} and larger of Mars atmosphere are for use within the atmosphere of Mars. These values include the effects of the 2π shadow shielding provided by the planet's bulk near its surface.

[13] For atmosphere path lengths and aluminum shielding thicknesses that are different than the values presented in Tables 1 and 2, interpolations or using curve fits to provide radiation exposure quantities for the unlisted, intermediate values is necessary and can be easily accomplished using numerical methods such as spline interpolations or by employing curve fitting software. The areal densities for the shielding provided by the combination of the atmosphere and aluminum can be determined for any point within the shielded geometry on the planetary surface using ray tracing techniques that adequately cover the 2π solid angle around the point in question (e.g., 1000 equally spaced rays).

4. Sample Results for a Mars Surface Scenario

[14] To illustrate use of the lookup tables, it is assumed that a crewmember is located at ground level in the center of a hemispherical shell structure composed of aluminum, which is located at the mean elevation of the surface of Mars. The ground level center location within the hemisphere is chosen because it is the point within the structure where the radiation exposures are the highest.

[15] For the pure CO_2 Mars atmosphere, both warm, low-density (16 g cm^{-2}) and cold, high-density (22 g cm^{-2}) models are available [*Smith and West*, 1983]. These areal densities are for the local zenith, the direction vertically through the Mars atmosphere starting from the mean surface elevation, and represent the thinnest shielding provided by the atmosphere. In this work we assume the warm, low-density model (16 g cm^{-2} of CO_2), which provides less atmospheric shielding.

Table 2. Mars Atmosphere Path-Length-Averaged Effective Dose for Galactic Cosmic Radiation

Aluminum Areal Density (g/cm^2)	Effective Dose (cSv/d)	Effective Dose Ratio[a]
1	0.06933	1.047
5	0.06856	1.035
10	0.06785	1.024
30	0.06624	1

[a]Ratio is effective dose (X g/cm^2)/effective dose (30 g/cm^2).

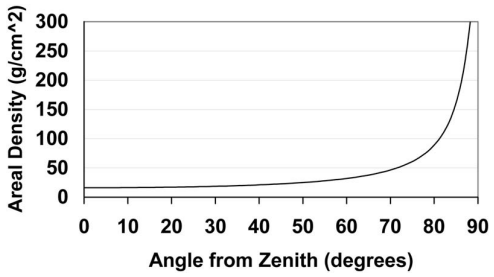

Figure 1. Mars atmosphere areal density (path length) as a function of arrival angle for the warm, low-density (16 g cm^{-2}) atmosphere model.

[16] Since incoming GCR radiation is isotropic, the atmosphere shielding thicknesses (path lengths) are greater for particles arriving at angles greater than zero, with respect to the local zenith. Therefore to account for this, the dose and effective dose must be averaged over all path lengths for all arrival angles from 0 to ~90 degrees. As the arrival angle approaches 90 degrees (the horizon), the areal densities increase dramatically, as seen in Figure 1, which displays the atmosphere path lengths for the warm, low-density atmosphere, as a function of arrival angle from 0 to ~90 degrees, as measured from the local zenith.

[17] To illustrate the use of the GCR lookup tables, we assume a hemispherical habitat on the Martian surface covered by the warm, low-density atmosphere. We also assume that incident spectrum is representative of the current 2009 environment (417 MV interplanetary magnetic field potential). Since the main radiation protection concern on the surface from incident GCR particles is the effective dose (acute radiation syndrome effects, such as radiation sickness, are not of concern since the absorbed doses are well below any threshold), we will focus on that radiation protection quantity in this work.

[18] Four areal densities for the aluminum hemisphere are assumed: 1 g cm^{-2}, 5 g cm^{-2}, 10 g cm^{-2} and 30 g cm^{-2}. These are selected because they are representative values

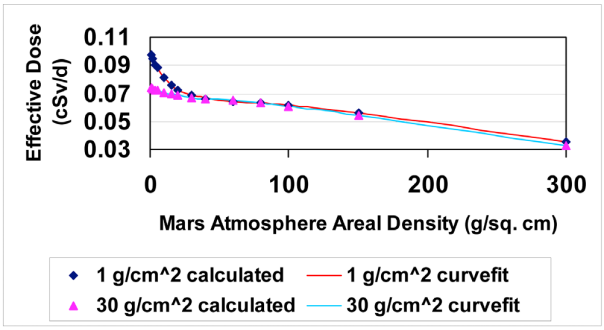

Figure 2. Effective dose (cSv/day) as a function of Mars atmosphere areal density for two different hemispherical aluminum habitat thicknesses (1 g cm^{-2} and 30 g cm^{-2}) for the 2009 GCR environment.

Table 3. Example Career Permissible Exposure Limits for Male Astronauts for a One Year Mission (NASA_STD_3001)

Age (Years)	Effective Dose (cSv)
25	52
30	62
35	72
40	80
45	95
50	115
55	147

for components that might become part of a constructed habitat. Figure 2 displays curves of the effective dose calculations for the 1 and 30 g cm^{-2} aluminum shields as a function of the atmosphere thickness obtained using a commercial curve-fitting software package (TableCurve 2D v5.01 software published by SYSTAT). Also displayed are the data points from the HZETRN calculations used for the curve fits. The curves for 5 and 10 g cm^{-2} aluminum shields are similar and lie between the two curves displayed in Figure 2.

[19] Table 2 displays the effective dose for each aluminum shield areal density after averaging over all path lengths (16 to 300 g cm^{-2}) for arrival angles of 0 to ~90 degrees from the zenith. These effective doses, extrapolated from daily values in Table 2 to annual values, range from 24.2 to 25.3 cSv. The NASA career exposure to radiation is limited to not exceed 3 percent risk of exposure induced death for fatal cancers. Table 3 lists the career permissible exposure limits for effective dose (in units of cSv) for a male crewmember for this guideline. Note that the effective doses in Table 2 are well below these limiting values, even for the youngest exposure age and for the smallest aluminum shield areal density. Note also, from Table 2, that the effective dose within the 1 g cm^{-2} aluminum shield is less than 5% higher than the effective dose within the 30 g cm^{-2} aluminum shield. Obviously, the presence of the overlying CO_2 atmosphere is the main source of shielding for the crew member on the surface. The presence of the aluminum shielding appears to have little effect on the effective dose.

[20] Nevertheless, to illustrate the use of the lookup tables for the GCR environment, a sector shield will be analyzed. Assume that a hemispherical habitat is shielded by 30 g cm^{-2} of aluminum for angles of 0 to 20 degrees from the zenith, by 10 g cm^{-2} of aluminum from 20 to 30 degrees, by 5 g cm^{-2} of aluminum from 30 to 45 degrees, and by 1 g cm^{-2} of aluminum from 45 to 90 degrees. Then the atmosphere-averaged effective dose, contributed by GCR particles arriving from all incident directions, for the assumed sector shield configuration, is 0.06652 cSv/d. This value is less than 0.5% higher than the value obtained with a complete, aluminum hemispherical shield with uniform areal density of 30 g cm^{-2}. As an alternate configuration, consider replacing the 5 and 10 g cm^{-2} aluminum shield sectors in the previous configuration with 1 g cm^{-2} of aluminum. The atmosphere-averaged effective dose is

0.06697 cSv/d, an increase of only 0.7%, over that of the original sectored configuration. To see the effect of using sectored shields on the total shield mass, rather than using a uniform areal density shield, recall that the total surface area of the hemisphere is $2\pi R^2$, where R is the radius of the hemisphere. For a sector ranging from zenith angles α to β, the surface area is

$$\textit{surface area} = 2\pi R^2 \int_{\alpha}^{\beta} \sin\theta \, d\theta = 2\pi R^2(\cos\alpha - \cos\beta) \quad (4)$$

and the mass of the sector segment is

$$\textit{shield mass} = (\textit{areal density}) \times (\textit{surface area}) \quad (5)$$

Hence, for a given hemispherical radius, the total mass of the sectored shield is

$$\textit{total mass} = \sum_i (\textit{segment mass})_i \quad (6)$$

Where the sum is over all of the different areal density segments.

[21] Using equations (4)–(6), the segment masses in the configuration utilizing all four areal densities are: (1) $3.6184\pi R^2$ for the 30 g cm^{-2} segment; (2) $1.4733\pi R^2$ for the 10 g cm^{-2} segment; (3) $1.5892\pi R^2$ for the 5 g cm^{-2} segment; and (4) $1.4142\pi R^2$ for the 1 g cm^{-2} segment. The total mass of shielding for the four areal density shield configuration is $8.0951\pi R^2$.

[22] For the alternate, two segment shield configuration, the segment masses are $3.6184\pi R^2$ for the 30 g cm^{-2} segment, and $1.8794\pi R^2$ for the 1 g cm^{-2} segment. The total mass of shielding for this configuration is $5.4978\pi R^2$, which is 32% lower, for an effective dose increase of only 0.7%.

5. Conclusions

[23] In this work the capabilities of the EMMREM framework to estimate GCR radiation exposures anywhere on the surface of Mars have been presented. To facilitate making estimates of human radiation exposures for crew operations in these scenarios, lookup tables have been generated that provide the means for obtaining estimates of doses for critical body organs and effective doses for exposures from GCR environments anywhere on the surface of Mars at any time during the solar cycle. A lookup table is used because the radiation environments are transported through as much as 500 g/cm^2 of atmosphere, aluminum and body self-shielding materials. Calculations at such depths for these complex space radiation environments cannot be carried out in near real time simulations. Methods of generating the lookup tables have been discussed and their use described. Sample calculations involving a simple, sector shielding configuration for a hemispherical, aluminum habitat on the surface of Mars were presented utilizing the lookup tables. The calculations demonstrate the effectiveness of the Mars atmosphere for shielding surface operations from GCR particles.

[24] **Acknowledgment.** Research support from the National Aeronautics and Space Administration, Living With a Star program, through grant NNX07AC14G is gratefully acknowledged.

References

Baker, D. N., et al. (2007), Space radiation hazards and the vision for space exploration: A report on the October 2005 Wintergreen Conference, *Space Weather*, *5*, S02004, doi:10.1029/2007SW000313.

Billings, M. P., and W. R. Yucker (1973), The computerized anatomical man (CAM) model, *NASA Contract. Rep.*, *CR-134043*.

Cucinotta, F. A., and M. Durante (2006), Cancer risk from exposure to galactic cosmic rays: Implications for space exploration by human beings, *Lancet Oncol.*, *7*, 431, doi:10.1016/S1470-2045(06)70695-7.

Hoff, J. L., L. W. Townsend, and E. N. Zapp (2002), Space radiation protection: Comparison of effective dose to bone marrow dose equivalent, *J. Radiat. Res.*, *43*, S125, doi:10.1269/jrr.43.S125.

Hoff, J. L., L. W. Townsend, and E. N. Zapp (2004), Interplanetary crew doses and dose equivalents: Variations among different bone marrow and skin sites, *Adv. Space Res.*, *34*, 1347, doi:10.1016/j.asr.2003.08.056.

Kim, M.-H. Y., F. A. Cucinotta, and J. W. Wilson (2007), A temporal forecast of radiation environments for future space exploration missions, *Radiat. Environ. Biophys.*, *46*(2), 95, doi:10.1007/s00411-006-0080-1.

Kim, M.-H. Y., M. J. Hayat, A. H. Feiveson, and F. A. Cucinotta (2009), Prediction of frequency and exposure level of solar particle events, *Health Phys.*, *97*(1), 68, doi:10.1097/01.HP.0000346799.65001.9c.

Lyne, J. E., and L. W. Townsend (1998), Critical need for a swingby return option for early manned Mars missions, *J. Spacecr. Rockets*, *35*, 855, doi:10.2514/2.7589.

NASA (2007), *NASA Space Flight Human System Standard*, vol. 1, *Crew Health, NASA-STD-3001*.

National Council on Radiation Protection and Measurements (1993), Limitation of exposure to ionizing radiation, *Rep. 116*, Bethesda, Md.

Nealy, J. E., F. A. Cucinotta, J. W. Wilson, F. F. Badavi, T. P. Dachev, B. T. Tomov, S. A. Walker, G. De Angelis, S. R. Blattnig, and W. Atwell (2007), Pre-engineering spaceflight validation of environmental models and the 2005 HZETRN simulation code, *Adv. Space Res.*, *40*, 1593, doi:10.1016/j.asr.2006.12.029.

O'Neill, P. M. (2006), Badhwar-O'Neill galactic cosmic ray model update based on Advanced Composition Explorer (ACE) energy spectra from 1997 to present, *Adv. Space Res.*, *37*, 1727, doi:10.1016/j.asr.2005.02.001.

Parsons, J. L., and L. W. Townsend (2000), Interplanetary crew dose rates for the August 1972 solar particle event, *Radiat. Res.*, *153*, 729, doi:10.1667/0033-7587(2000)153[0729:ICDRFT]2.0.CO;2.

PourArsalan, M., L. W. Townsend, N. A. Schwadron, K. Kozarev, M. A. Dayeh, and M. I. Desai (2010), Time-dependent estimates of organ dose and dose equivalent rates for human crews in deep space from the 26 October 2003 solar energetic particle event (Halloween event) using the Earth-Moon-Mars Radiation Environment Module, *Space Weather*, *8*, S00E05, doi:10.1029/2009SW000533.

Saganti, P. B., F. A. Cucinotta, J. W. Wilson, L. C. Simonsen, and C. Zeitlin (2004), Radiation climate map for analyzing risks to astronauts on the Mars surface from galactic cosmic rays, *Space Sci. Rev.*, *110*, 143, doi:10.1023/B:SPAC.0000021010.20082.1a.

Schwadron, N. A., et al. (2010), Earth-Moon-Mars Radiation Environment Module framework, *Space Weather*, *8*, S00E02, doi:10.1029/2009SW000523.

Shinn, J. L., J. E. Nealy, L. W. Townsend, J. W. Wilson, and J. S. Wood (1994), Galactic cosmic ray radiation levels in spacecraft on interplanetary missions, *Adv. Space Res.*, *14*, 863, doi:10.1016/0273-1177(94)90551-7.

Simonsen, L. C., J. E. Nealy, L. W. Townsend, and J. W. Wilson (1990), Space radiation dose estimates on the surface of Mars, *J. Spacecr. Rockets*, *27*, 353, doi:10.2514/3.26149.

Simonsen, L. C., J. E. Nealy, L. W. Townsend, and J. W. Wilson (1991), Martian regolith as space radiation shielding, *J. Spacecr. Rockets*, *28*, 7, doi:10.2514/3.26201.

Smith, R. E., and G. S. West (1983), *Space and Planetary Environment Criteria Guidelines for Use in Space Vehicle Development: 1982 Revision*, *NASA Tech. Memo.*, *TM-82478*, vol. 1, 300 pp.

Townsend, L. W. (2005), Implications of the space radiation environment for human exploration in deep space, *Radiat. Prot. Dosim.*, *115*, 44, doi:10.1093/rpd/nci141.

Townsend, L. W., J. E. Nealy, J. W. Wilson, and W. Atwell (1989), Large solar flare radiation shielding requirements for manned interplanetary missions, *J. Spacecr. Rockets*, *26*, 126, doi:10.2514/3.26043.

Townsend, L. W., J. L. Shinn, and J. W. Wilson (1991), Interplanetary crew exposure estimates for the August 1972 and October 1989 solar particle events, *Radiat. Res.*, *126*, 108, doi:10.2307/3578178.

Townsend, L. W., F. A. Cucinotta, and J. W. Wilson (1992), Interplanetary crew exposure estimates for galactic cosmic rays, *Radiat. Res.*, *129*, 48, doi:10.2307/3577902.

Townsend, L. W., F. A. Cucinotta, J. W. Wilson, and R. Bagga (1994), Estimates of HZE particle contributions to SPE radiation exposures on interplanetary missions, *Adv. Space Res.*, *14*, 671, doi:10.1016/0273-1177(94)90524-X.

Townsend, L. W., D. L. Stephens Jr., J. L. Hoff, E. N. Zapp, H. M. Moussa, T. M. Miller, C. E. Campbell, and T. F. Nichols (2006), The Carrington event: Possible doses to crews in space from a comparable event, *Adv. Space Res.*, *38*, 226, doi:10.1016/j.asr.2005.01.111.

Townsend, L. W., Y. M. Charara, N. Delauder, M. PourArsalan, J. A. Anderson, C. M. Fisher, H. E. Spence, N. A. Schwadron, M. J. Golightly, and F. A. Cucinotta (2010), Parameterizations of the linear energy transfer spectrum for the CRaTER instrument during the LRO mission, *Space Weather*, *8*, S00E03, doi:10.1029/2009SW000526.

Zapp, E. N., L. W. Townsend, and F. A. Cucinotta (2002), Solar particle event organ doses and dose equivalents for interplanetary crews: Variations due to body size, *Adv. Space Res.*, *30*, 975, doi:10.1016/S0273-1177(02)00166-7.

F. A. Cucinotta and M. Y. Kim, NASA Lyndon B. Johnson Space Center, Houston, TX 77058, USA.

M. PourArsalan and L. W. Townsend, Department of Nuclear Engineering, University of Tennessee, Knoxville, TN 37996-2300, USA. (ltownsen@utk.edu)

N. A. Schwadron, Department of Astronomy, Boston University, Boston, MA 02215, USA.